Role of zinc and magnesium ions in the modulation of phosphoryl transfer in protein tyrosine phosphatase 1B

Elisa Bellomo,[a] Asma Abro,[b] Christer Hogstrand,[a] Wolfgang Maret[a,*] and Carmen Domene[b,c,d*]

[a] Departments of Biochemistry and Nutritional Sciences, King's College London, 150 Stamford Street, London, SE1 9NH, UK, [b] Department of Chemistry, King's College London, Britannia House, 7 Trinity Street, London SE1 1DB, UK, [c] Chemistry Research Laboratory, Mansfield Road, University of Oxford, Oxford OX1 3TA, UK, [d] Department of Chemistry, University of Bath, 1 South Building, Claverton Down, Bath BA2 7AY, UK

ABSTRACT: Whilst the majority of phosphatases are metalloenzymes, the prevailing model for the reactions catalyzed by protein tyrosine phosphatases does not involve any metal ion. Yet, both metal cations and oxoanions affect their enzymatic activity. Mg^{2+} and Zn^{2+} activate and inhibit, respectively, protein tyrosine phosphatase 1B (PTP1B). Molecular dynamics simulations, metadynamics and quantum chemical calculations in combination with experimental investigations demonstrate that Mg^{2+} and Zn^{2+} compete for the same binding site in the active site only in the closed conformation of the enzyme in its phosphorylated state. The two cations have different effects on the arrangements and activities of water molecules that are necessary for the hydrolysis of the phosphocysteine intermediate in the second catalytic step of the reaction. Remarkable differences between the established structural enzymology of PTP1B investigated ex vivo and the function of PTP1B in vivo become evident. Different reaction pathways are viable when the presence of metal ions and their cellular concentrations are considered. The findings suggest that the substrate delivers the inhibitory Zn^{2+} ion to the active site. The inhibition and activation can be ascribed to the different coordination chemistry of Zn^{2+} and Mg^{2+} ions and the orientation of the metal-coordinated water molecules. Metallochemistry adds an additional dimension to the regulation of PTP1B, and presumably other members of this enzyme family.

Introduction

The remarkable catalytic efficiency of enzymes is based on multiple intermediates and conformational states.[1] With movements of polypeptide segments looping around the active site and several amino acid side chains involved in two catalytic steps, protein tyrosine phosphatases (PTPs) are no exception. The conformational landscape of their active sites is quite diverse because some of them need plasticity for broad substrate specificity in accepting several client proteins. Their catalytic mechanism has been investigated in detail with special reference to PTP1B, an enzyme that controls the dephosphorylation and hence signalling of the insulin receptor (Scheme 1).[2] A key aspect of its 3D structure is a transition from an open to a closed conformation. In this process, a movement of the so-called WPD loop occurs, shifting residues up to 8 Å during substrate binding and bringing the catalytic Asp181 into a position for proton transfer. The phosphatase reaction involves the catalytic Cys215, which is not part of the WPD loop. The cysteine thiol has an unusually low pK_a of 5.5.[3] In the first step of the reaction, the cysteine thiolate forms

a covalent cysteinylphosphate intermediate with the phosphate group cleaved from the phosphotyrosine-containing substrate, resulting in the first product, the dephosphorylated substrate. Arg221 interacts with the cysteinylphosphate through two hydrogen bonds. The leaving group (the tyrosinate of the substrate) is protonated by Asp181, which is thought to have an unusually high pK_a of 6.8. The second, rate-limiting step is the hydrolysis of the cysteinylphosphate intermediate. It is thought to involve a water molecule as a nucleophile. The water molecule binds to the cysteinylphosphate, forming an O-P bond and breaking the P-S bond, resulting in a Walden inversion during the S_N2 process.[4] The role of amino acids in this step is not entirely clear. The water molecule is thought to interact with Asp181 and Gln266 based on the characterization of a cysteinylphosphate intermediate of PTP1B, in which Gln266 had been replaced with an Ala.[5] Gln266 has been described as a catalytic residue, but it is thought to participate in alignment and not activation of the water molecule critical for bond cleavage. The role of Asp181 in the second transition state (TS) is thought to be in hydrogen bonding to the phosphate dianion and to serve as the general base, accepting a proton from the water molecule. This mechanism was suggested from density functional theory (DFT) calculations for a low molecular mass PTP (BPTP), where the deprotonated state of the relevant Asp residue predominates in the free enzyme at neutral pH (pK_a = 5.3).[6] Overall, aspects of this mechanism are in agreement with crystal structures of the enzyme in the open and closed conformation, its two TSs, and its Michaelis-Menten complexes.[2]

Scheme 1. Proposed catalytic cycle and reaction mechanism.

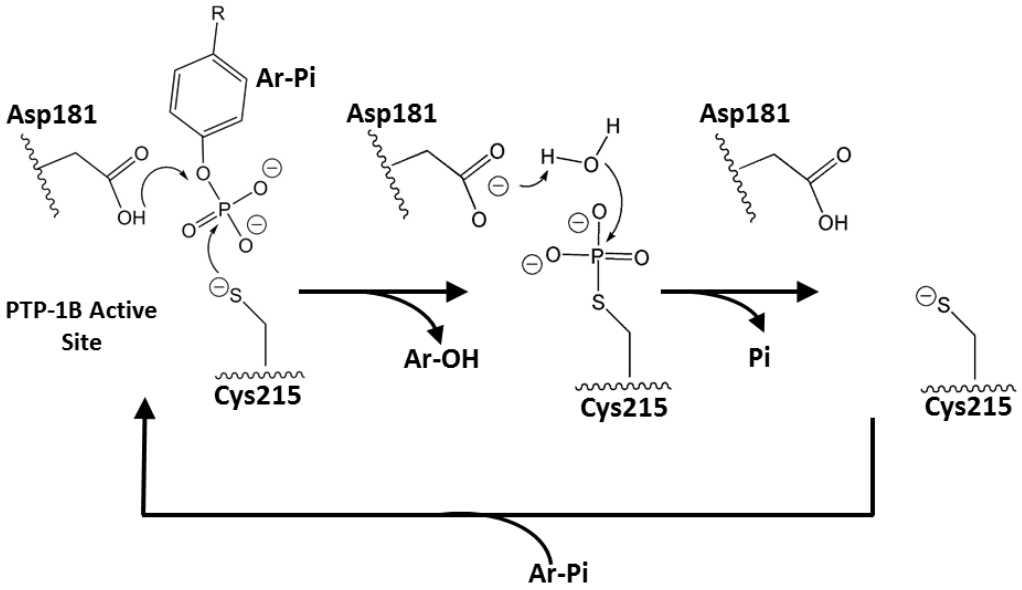

Remarkably, metal ions are absent in this mechanism and consequently PTPs were thought not to require metal ions for their enzymatic activity. However, zinc ions were identified almost 40 years ago as inhibitors of PTP1B.[7] More recently, inhibition constants in the nanomolar or even picomolar range were

determined for PTPs, suggesting that zinc ions are physiological modulators of PTP-catalyzed reactions.[8,9] Enzyme kinetics suggested that zinc inhibition occurs in the closed conformation of the enzyme when the catalytic cysteine (Cys215) is phosphorylated. Molecular docking experiments suggested Asp181 and the phosphate group of the cysteinylphosphate as ligands of the inhibitory zinc ion.[8] Based on the observation reported here that magnesium ions activate PTP1B, the objective of the present investigation was to further examine the role of magnesium and zinc ions in PTP1B catalysis.

Materials and Methods

The cDNA of the cytoplasmic domain of human PTP1B was kindly provided by Dr Alastair Barr (University of Westminster, UK). PTP1B was prepared and purified as described[10] by Dundee Cell Products (https://www.dundeecellproducts.com/). Insulin receptor (IR) peptides were purchased from Enzo Life Sciences. Four peptides containing the sequences of amino acids 1142-1153 of the insulin receptor were used: the dephosphorylated peptide (IR, Thr-Arg-Asp-Ile-Tyr-Glu-Thr-Asp-Tyr-Tyr-Arg-Lys), and the three phosphorylated peptides containing either one (1pY-IR, Thr-Arg-Asp-Ile-pTyr-Glu-Thr-Asp-Tyr-Tyr-Arg-Lys), two (2pY-IR, Thr-Arg-Asp-Ile-pTyr-Glu-Thr-Asp-pTyr-Tyr-Arg-Lys), or three phosphotyrosines (3pY-IR, Thr-Arg-Asp-Ile-pTyr-Glu-Thr-Asp-pTyr-pTyr-Arg-Lys).

Enzymatic assays

PTP1B activity was assayed fluorimetrically at 25 °C in a freshly prepared buffer containing 50 mM Hepes/Na^+, pH 7.4, 0.1 mM tris(2-carboxyethyl)phosphine (TCEP) with or without 1 mM nitrilotriacetic acid (NTA), and 0.01% (v/v) Triton X-100 ('assay buffer'). The enzyme was added to the buffer to a final concentration of 5 nM and the mixture incubated for five minutes. The reaction was initiated by adding the fluorogenic phosphatase substrate 6,8-difluoro-4-methylumbelliferyl phosphate (DiFMUP). Assays were performed in triplicates in a total volume of 100 µl in 96-well black optical bottom plates (Greiner Bio-One Ltd, Stonehouse, UK). Product formation (hydrolysis of DiFMUP to 6,8-difluoro-7-hydroxy-4-methylcoumarin) was monitored by fluorescence at 460 nm with 360 nm excitation using a plate reader (Synergy HT, BioTek, Winooski, VT). The initial rate was determined from the linear portion of the progress curves.

The effect of zinc ions on PTP1B was determined by enzymatic assays.[8] Briefly, increasing concentrations of $ZnSO_4$ were added to the assay buffer and the mixture left to equilibrate for 15 minutes. The effect of magnesium ions was determined by adding increasing concentrations of $MgSO_4$ to the assay buffer without NTA and with the same equilibration before adding PTP1B. The initial rate was determined from the linear portion of the progress curves and plotted as percentage of control (without added metal ions).

Fluorescence of peptides

Fluorescence emission spectra of 10 μM insulin receptor peptides (excitation 280 nm) in assay buffer were recorded (Figure S1) in the absence and presence of 1 mM $ZnSO_4$ at 23 ^{o}C with a Perkin Elmer LS50B spectrofluorimeter (Bucks, UK).

Classical Molecular Dynamics simulations

The starting models for molecular dynamics (MD) simulations of PTP1B were the deposited crystallographic protein structures with PDB ID 2CMC (open conformation) and 3I80 (second TS, closed conformation), respectively. The conformation of the cysteinylphosphate intermediate of PTP1B was modelled using the structure 1A5Y (closed conformation) that had been crystallized by mutating the active site residue Gln262 into Ala. The first TS was modelled using the structure 3I7Z. PTP1B crystal structures show water molecules surrounding active site residues Asp181 and Cys215 in all three conformational states.

In simulation sets 23 and 24 from Table S1, the Gln262 to Ala mutation was reverted to investigate binding of divalent metal ions using a catalytically competent protein model. Meta- and orthovanadate, which mimic the phosphate group in the TSs and are present in the crystal structures, were not considered in the simulations.

Default protonation states were considered for ionizable residues with the exception of Asp181, which was modelled either neutral (protonated) or negatively charged. All histidine residues were modelled in their neutral form with the hydrogen atom at the epsilon position. Systems were solvated and $ZnCl_2$ or $MgCl_2$ was added to achieve neutralization of the system up to a final concentration of 150 mM.

The NAMD software[11] was used with the CHARMM 27 force field[12] and CMAP corrections for the classical MD simulations. The TIP3P model[13] was used for water, and the standard CHARMM parameters for ions. Parameters for the cysteinylphosphate in the covalent intermediate were developed in-house (Supplementary Material). Parameters were assigned by dividing the molecule in its molecular components. A search for corresponding (or homologue) parameters in the CHARMM general force field (CGenFF)[14] was performed. For the sulphur-phosphorus bond, no parameters were available in the CGenFF. Parameterization was undertaken using the force field Tool Kit (FFTK).[15]

Each system was initially energy minimized (2000 steps) and equilibrated to remove initial steric clashes (50 ps, 1 fs time step). Subsequently, production simulations were performed in the NpT ensemble. Semi-isotropic pressure coupling at 1 atm was accomplished using the Nosé-Hoover Langevin piston,[16,17] while temperature control was achieved by means of the Langevin thermostat.[18] Long range electrostatic interactions were treated using the particle mesh Ewald algorithm,[19] and van der Waals forces were

smoothly switched off at 10-12 Å. The SHAKE algorithm was used to constrain all bonds involving hydrogen atoms in order to use a timestep of 2 fs. Non-bonded short and long-range interactions were computed every time step. Initial structures with docked ions were obtained from published results.[8] Details of all systems considered in this investigation are presented in Table S1. The total simulation time was ~4 μs.

Metadynamics simulations to study substrate binding

Ion access to the PTP1B active site via coordination to a substrate molecule was tested computationally. In particular, the metadynamics approach[20] implemented in the NAMD software package[11] was employed. Two independent MD simulations of PTP1B in complex with a substrate molecule (DiFMUP) and Zn^{2+}/Cl^{-} or Mg^{2+}/Cl^{-} ions were considered. An equilibration protocol identical to the one described previously was used, with production runs of 40 ns in the NpT ensemble. Weak spatial constraints were added to the substrate molecule, initially placed in the solution, to allow free interaction with Zn^{2+} or Mg^{2+} but preventing entrance into the active site of PTB1B. During this time, Zn^{2+} or Mg^{2+} binds to the DiFMUP substrate molecule. In particular, Zn^{2+} shows high affinity for DiFMUP with formation of a stable complex at approximately 7 ns whereas Mg^{2+} interacts less tightly with the formation of transient complexes at 16 and 38 ns.

Representative snapshots of the MD simulations were taken as starting points of the metadynamics simulations. Two collective variables were chosen and they are illustrated in Scheme 2A. The first collective variable (CV1) measures the degree of penetration of the substrate into the active site; this was defined as the distance between the center of mass of the phosphate in DiFMUP and the center of mass of the nucleophile residue of the protein (Cys215). The second collective variable (CV2) accounts for the formation of a hydrogen bonding interaction between the substrate and the acid/base residue, and it was defined as the distance between the center of mass of phosphate in DiFMUP and the center of mass of the acid/base Asp181 side-chain residue. The values of the height and width of the Gaussian-like potentials employed were selected to be 1.0 kcal/mol and 0.15 Å (CV1) and 0.25 Å (CV2), respectively. A new Gaussian potential was added every 1 ps. Reflective walls were placed at distances of 16 Å and 25 Å for CV1 and CV2, respectively. Once the systems had explored several times the free-energy surface, which in terms of simulation time corresponds to approximately 300 ns, the runs were stopped.

Scheme 2. Reaction mechanism of PTP1B. Diagrammatic representation of the collective variables employed for (A) the metadynamics simulations used to study substrate binding, and (B) the QM/MM MD simulation to study the enzymatic reaction. DiFMUP is a fluorescent substrate of PTP1B.

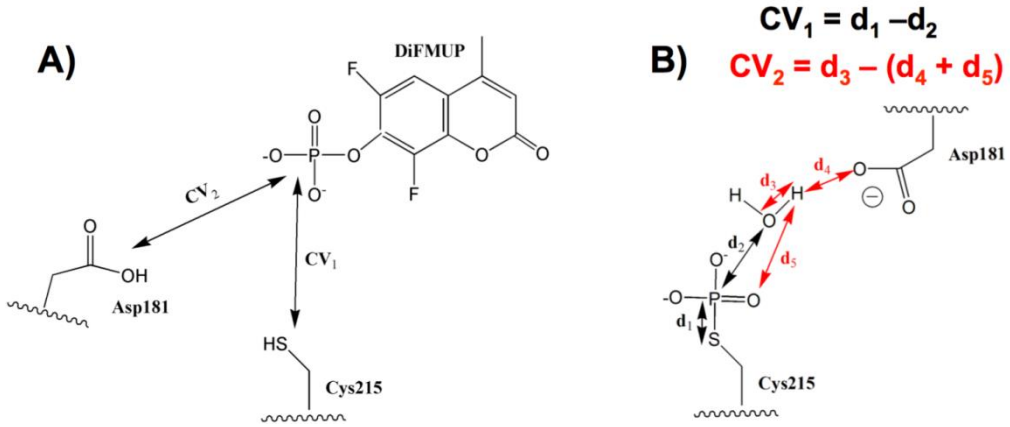

QM/MM MD and metadynamics simulations to study the reaction mechanism

To assess the role of Zn^{2+} and Mg^{2+} in the modulation of the second step of the PTP1B-catalyzed reaction, dephosphorylation of PTP1B was modelled using the enzyme in the presence of each ion. A snapshot of the cysteinylphosphate intermediate from the classical MD simulation was used as starting structure. A water molecule interacting with the phosphate group was 'manually' replaced by either Zn^{2+} or Mg^{2+} to obtain the metal-bound systems. The systems were subsequently equilibrated during 5 ns of classical MD simulation. In order to obtain an accurate description of the enzymatic reaction, a QM/MM approach was employed using the driver implemented in the CP2K package.[21] The QM region was treated at the density functional theory (DFT) level of theory with a triple-zeta valence basis set with two sets of polarization functions, TZV2P.[22] A cut-off of 350/450 Ry for the auxiliary plane-wave basis set was used for the protein and ions, respectively. Godecker, Teter and Hutter (GTH) pseudopotentials[23,24] were used for describing the core electrons and nuclei, together with the gradient-corrected Becke exchange[25] and the Lee, Parr, and Yand correlation functional (BLYP).[26] A cubic QM cell size of 18 Å was selected based on the energy convergence with respect to the wave function gradient (5×10^{-7} Hartree) for all the systems studied. For the enzyme, the QM region consists of the side chains of Asp181 and the phosphorylated Cys215, and three water molecules interacting with the phosphate group. The Mg^{2+}/Zn^{2+} QM regions consist of Asp181, phosphorylated Cys215, the corresponding ion and the solvation shell of the ion. The boundary between the QM and MM regions (C_α-C_β in Asp181 and Cys215) was saturated using the IMOMM link scheme[27] and the MM region was treated at the classical level with the CHARMM force field. Each QM/MM simulation was equilibrated for 20 ps.

Subsequently, the metadynamics approach was used to describe the reaction mechanism of PTP1B. In this case, two collective variables also were chosen to track the main bonds involved in the reaction (Scheme 2B). The first collective variable (CV1) describes the nucleophilic attack of a water molecule on the cysteinylphosphate intermediate. It is defined as the difference between two bond distances [CV1 = d_1 –

d_2], where d_1 is the distance between the S and P atoms in residue Cys215, and d_2 is the distance between the P atom of residue Cys215 and the oxygen of the water molecule considered in the reaction. Therefore, this collective variable accounts for the nucleophilic attack of the water molecule and phosphate release. The second collective variable (CV2) describes the proton transfer between the water molecule, the Asp181 residue, and the phosphate molecule, and is also defined as a combination of three bond distances [$CV2 = d_3 – (d_4 + d_5)$].

The metadynamics calculation was performed using repulsive Gaussian-shaped potentials with a height of 1.5 kcal/mol and a width of 0.2 Å and 0.1 Å for CV1 and CV2, respectively. A new Gaussian potential was added every 40 QM/MM MD steps (20 fs). To restrict the surface to be explored, an upper limit in the CV1 space was imposed at 3.5 Å, with a quadratic potential constant of 20 kcal/(mol Å^2) and CV2 was delimited by two quadratic walls at –4.5 and 4.5 Å, with a quadratic potential constant of 20 kcal/(mol·Å^2). The systems were evolved for ~90 ps when they showed free diffusion along the collective variables.

Further geometry optimization of the reactants and TS structures extracted from the metadynamics simulations for Mg^{2+}/Zn^{2+} systems was performed using CP2K. The Mg^{2+}/Zn^{2+} QM region consisted of the side chain of Asp181 and phosphorylated Cys215, the ion and its solvation shell. The boundary between the QM and MM regions (C_α-C_β in Asp181 and Cys215) was saturated using the IMOMM link.[27] A schematic representation of the protocol followed to investigate the Zn^{2+}/Mg^{2+} ion coordination to PTP1B in the CSP intermediate is shown in Figure S4. Results are depicted in Figure S5 for optimization of reactant state and TS, as well as representative snapshot from production runs.

Results and Discussion

Opposite effects of zinc and magnesium on PTP1B activity

When increasing concentrations of Zn^{2+} or Mg^{2+} were added to PTP1B and the enzymatic activity determined, zinc inhibited with an IC_{50} value of 3-15 nM as reported previously,[28] but magnesium activated with an EC_{50} value of 41 μM (Figure 1A,B). Since neither zinc nor magnesium ions have been implicated in the reaction mechanism of this enzyme their role was further examined.

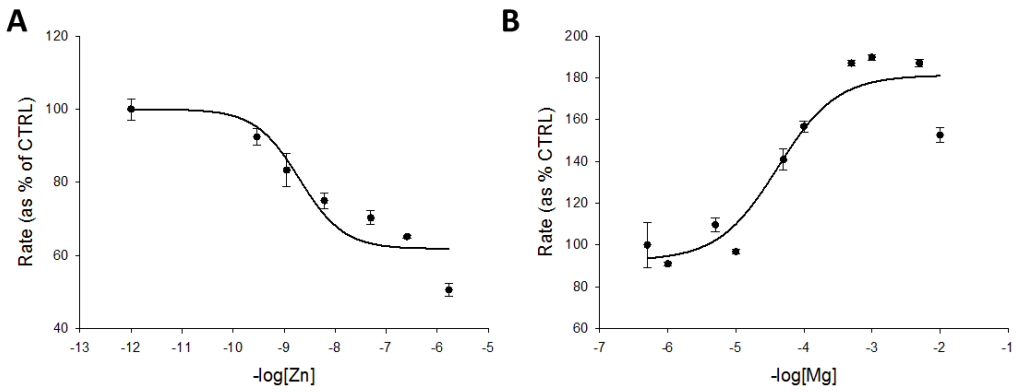

Figure 1. Zinc and magnesium ions affect PTP1B enzymatic activity. The enzymatic activity of PTP1B was tested at increasing concentrations of buffered (A) zinc or (B) magnesium ions in the presence of 50 mM Hepes, pH 7.4 and 1 mM NTA (included only when zinc was examined), 0.1 mM TCEP, and 0.01% Triton X-100. n=3.

Classical Molecular Dynamics simulations to study metal ion binding to PTP1B

To obtain insight into how the metal ion gains access to the PTP1B active site, binding of magnesium or zinc ions to PTP1B in the open, closed and covalent intermediate structures was analyzed using classical MD simulations. The results show Zn^{2+} binding at the surface of the protein in all conformations (Figure S2). When ions were placed at random positions in the simulations box, the number of binding sites was reduced to three. Based on previous nomenclature used in molecular docking experiments,[8] they correspond to binding sites 1, 4, and 6 (Figure S2). In contrast, MD simulations starting with docked metal ions[8] resulted in a higher number of metal ion binding sites. Specifically, six binding sites were characterized (binding sites 2, 3, 5, 7, 8, and 10; Figure S2), suggesting that longer simulations times are required to reach stable bound configurations. There is a caveat, however, in the interpretation of these results, namely that, despite the success of the classical additive force fields, fixed charge models present a series of limitations, including that they are ineffective when describing situations with large electrostatic polarization effects such as in PTP1B's active site.[29] In contrast to Zn^{2+}, a scattered pattern of Mg^{2+} was observed at the protein surface. It is indicative of random movements of the ions and weaker interactions with the protein. Binding of Mg^{2+} or Zn^{2+} at the active site was not observed during these timescales. Identical analysis was performed on the MD trajectories of the closed conformation of PTP1B in the presence of Mg^{2+} or Zn^{2+}. The behaviour of the zinc ions was almost identical to the one observed in the open conformation. Significantly, a docked ion remains bound to the acid/base residue Asp181 (Binding site 11; closed conformation, Figure S2). However, it is exposed to the solvent and does not enter the binding site proposed from molecular modelling. Mg^{2+} is not as tightly bound to the protein surface as Zn^{2+} in the simulations of the covalent intermediate.

As metal ion binding was not observed at the active site of the enzyme at the timescales used, we investigated the effect of the different protonation states of the side chain of residue Asp181, which serves as the catalytic acid/base. Its protonation state is affected by the conformational state of the protein. The closed conformation of the enzyme is maintained when Asp181 is in its protonated form, while Asp181 is thought to be deprotonated in the open conformation.[3] The additional simulations did not result in any metal ion binding at the active site despite the presence of a negative electrostatic field in some cases, which might have had some effect on attracting the cation to the active site.

In summary, the results show Zn^{2+} binding to the PTP1B surface in the open and closed conformations, as well as in the cysteinylphosphate intermediate. The presence of several binding sites that were not conserved among simulations can be attributed to sampling limitations. In contrast to rigid molecular docking calculations,[10] ion binding was not observed at the catalytic site in the covalent intermediate. This result, together with the absence of ion diffusion to the active site in the simulations of the open and closed PTP1B conformations, raised the question of whether or not ions rely on a phosphorylated substrate to enter the active site of the enzyme. Therefore, zinc binding to a PTP1B substrate was investigated.

Zinc interacts with a PTP1B substrate

$ZnSO_4$ up to a final concentration of 1 mM was added to the four insulin receptor peptides (IR1142-1153) and fluorescence spectra were acquired every minute to measure the time-dependent effects of zinc on the peptides. At the end of the experiment, 5 mM EDTA was added to examine reversibility of effects attributed to zinc binding. Zinc decreased the intrinsic fluorescence of the partially dephosphorylated forms of the peptides, the monophosphorylated 1pY-IR and the diphosphorylated 2pY-IR, only marginally (Figure S1). However, it increased the fluorescence of the peptide containing three phosphotyrosines (3pY-IR). This result demonstrates zinc binding to the insulin receptor peptides with three phosphotyrosines (Figure 2). Indeed, zinc inhibition of PTP1B is not the only effect of zinc on insulin signaling as an interaction between the insulin receptor and zinc also has been reported.[30]

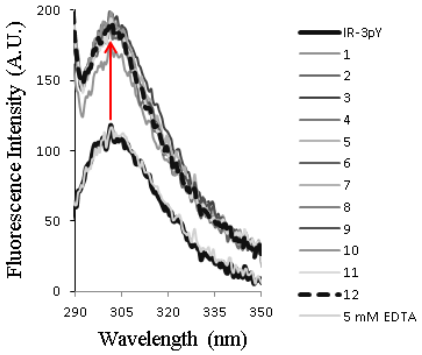

Figure 2. Zinc alters the intrinsic fluorescence of a phosphorylated insulin receptor (IR) peptide. 1 mM $ZnSO_4$ was added to 10 μM of IR peptide containing phosphotyrosines. The sample was excited at 280 nm and emission spectra were collected a minute after zinc addition.

Ability of DiFMUP to bind metal ions and entrance into the PTP1B active site

Conformational changes are often rate-limiting to enzymatic turnover regarding product release because chemical steps are usually much faster.[31,32] Here, direct participation of molecular motions in the chemical steps of the enzymatic reaction[31] was tested. To this end, classical MD simulations coupled to the metadynamics approach were employed to characterize the role of structural motions of key segments of the enzyme, namely the P-loop, the WPD-loop, the Q-loop, the Lys-loop and the Tyr recognition loop. These loops have different functions. The P-loop is composed of residues 215-222, which include the catalytic Cys215, Ser222 that stabilizes its thiolate form and Arg221 involved in binding and TS stabilization. The general acid-base residue, Asp181, belongs to the WPD-loop, which is composed of residues 179-187 and alternates between open and closed conformations. It is thought to play a crucial role in the activation mechanism and interaction with Lys120 in the Lys-loop (residues 119-121). Residues 47-49 define the Tyr recognition loop involved in recognition and binding of substrate. Finally, the Q-loop, which is composed of residues 261 and 262, is involved in the second catalytic step.[2]

Computations to simulate the process by which the substrate DiFMUP enters the active site of PTP1B were undertaken. Two independent metadynamics simulations of PTP1B in the presence of DiFMUP and Zn^{2+} or Mg^{2+} were performed (Figure 3). Both free energy surfaces of ligand binding obtained from the metadynamics simulations show a broad energy minimum in which a DiFMUP-ion complex is inside the active site of the enzyme (structures labelled M1/M2 or M1b/M2b). Close examination of both energy minima reveals different conformations of the WPD-loop containing the catalytic residue Asp181. Energy minima M2 and M2b correspond to conformations in which the catalytic residue is far from the substrate and proton transfer cannot occur. In contrast, in the M1 and M1b minima, the side chain of Asp181 points toward the phosphate group of the substrate and is in hydrogen bonding distance, consistent with its role as a proton donor. Furthermore, Zn^{2+} or Mg^{2+} are bound to the substrate at each step of the entry process, confirming the hypothesis that divalent metal ions enter the active site of the enzyme when bound to the substrate.

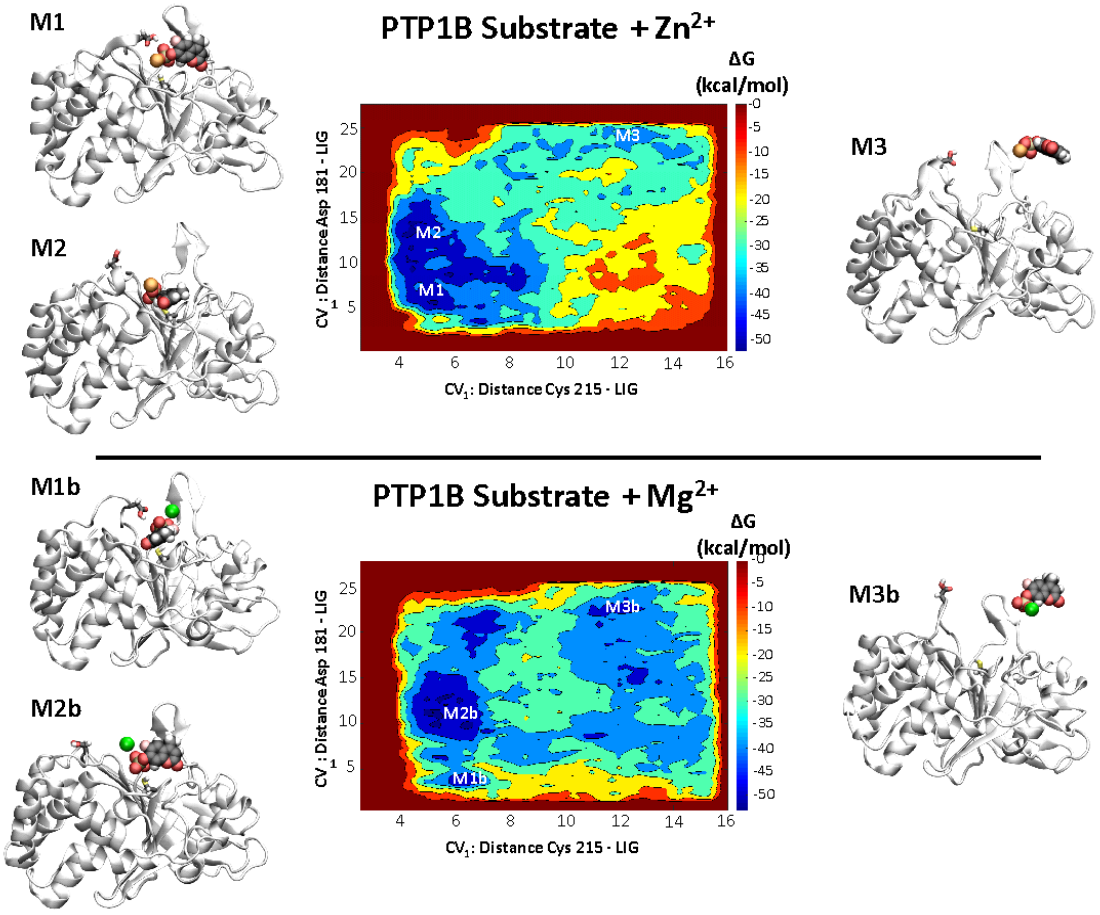

Figure 3. Metadynamics simulations to investigate DiFMUP substrate entry to the catalytic site of PTP1B. Free energy maps were obtained from metadynamics simulations using two collective variables as described in the main text. Contour lines are presented for every 10 kcal/mol. Energy minima are labelled as M1, M2, and M3 for the simulations with Zn^{2+} and M1b, M2b, and M3b for the simulations with Mg^{2+}. The protein structure is presented as a solid white surface, whereas catalytic residues Asp181 and Cys215, the substrate molecule and interacting ions are shown as Van der Waals spheres. C, O, H, S, Zn and Mg atoms are shown in black, red, white, yellow, orange and green, respectively.

These results are in agreement with experimental observations that the tuning of loop motion is closely synchronized with hydrolysis of phosphotyrosine and coupled to the protonation of the tyrosine leaving group.[31] In this way, phosphorylation of the enzyme or dephosphorylation of the substrate are modulated at different levels by controlling the kinetics of the P-loop.

QM/MM metadynamics simulations to investigate the effect of metal ions on the PTP1B enzymatic reaction

PTP1B remained at least 50% active even in the presence of high Zn^{2+} concentrations under the same assay conditions employed to investigate the effect of Mg^{2+} (Figure 1). The dephosphorylated substrate is released in the first catalytic step of the reaction and the retention of activity suggests that the enzyme is

inhibited in the second catalytic step, when the enzyme is still in its phosphorylated form. To elucidate the effects of metal ions on the enzymatic activity and investigate how Zn^{2+} and Mg^{2+} are coordinated in the active site, hybrid quantum mechanics/molecular mechanics simulations (QM/MM) and free energy calculations were performed to reconstruct the second catalytic step of the reaction using PTP1B in the presence of Zn^{2+} or Mg^{2+} bound to the cysteinylphosphate intermediate. Starting from a structure of the enzyme equilibrated by means of classical MD simulations, a water molecule bound to the phosphate group was 'manually' replaced by Zn^{2+} or Mg^{2+}. Energy minimization followed by 5 ns of classical MD simulations lead to octahedral coordination of both ions. When 20 ps of production runs were collected the coordination number of Zn^{2+} changed from octahedral to tetrahedral while Mg^{2+} retained its octahedral coordination (Figure 4). These results are in agreement with the expected coordination chemistry of the two ions and with experimental observations.[33] The different coordination numbers of each ion arrange the water molecules in the vicinity of the phosphate group differently, with the nearest water molecule being at 3.35 Å and 3.74 Å from Mg^{2+} and Zn^{2+}, respectively, as compared to 3.48 Å from the active site in the absence of ions. Thus, Mg^{2+} and Zn^{2+} orient the reactive water molecules in positions that are either more or less suitable to perform the nucleophilic attack on the phosphorylated cysteine, demonstrating their opposite effects, namely activation by Mg^{2+} and inhibition by Zn^{2+}.

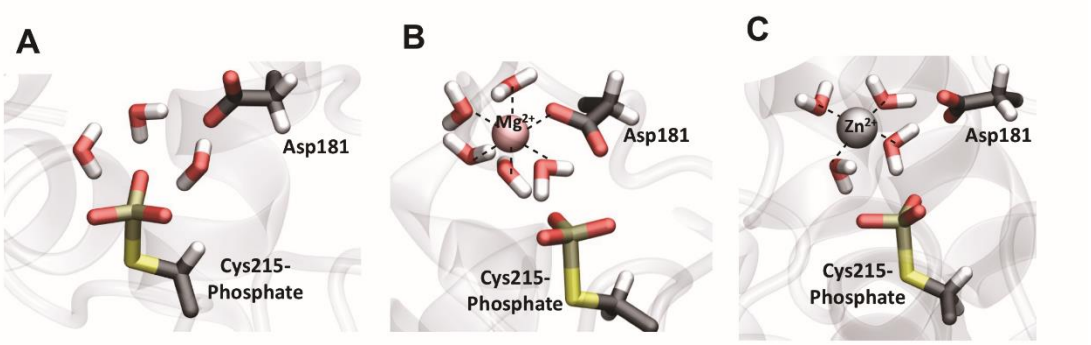

Figure 4. The active site of PTP1B in a representative snapshot at the end of the QM/MM MD simulations. (A) Structure in the absence of metal ions, and (B) Mg^{2+} and (C) Zn^{2+} bound systems. Residues Cys215phosphate, Asp181 and water molecules in the active site or coordinating the metal are shown in licorice representation. C atoms are depicted in black, S atoms in yellow, O atoms in red and H atoms in white. Protein secondary structural elements are shown as white transparent surfaces.

To investigate the reaction mechanism of PTP1B at the molecular level and the effects of metal ion binding in the active site, the free energy surface (FES) of the process was reconstructed as a function of two collective variables (Materials and Methods) (Figure 5). The FES for the reaction of PTP1B shows a broad minimum corresponding to the reactants (R) and two minima for the product states (P and P'), differing in the protonation state of the Asp181 residue and the phosphate group. In the TS of the reaction, the S-P bond is partially broken, with the adoption of a trigonal bipyramidal geometry for the phosphate

group; a water molecule approaches the phosphorous atom to perform the nucleophilic attack. The product (P) resulting from the transfer of a proton from Asp181 to the hydrolyzed phosphate is higher in stability than P' by approximately 5 kcal/mol. The PTP1B reaction is exothermic with a total free energy change of 4 kcal/mol and a free energy barrier of 18 kcal/mol.

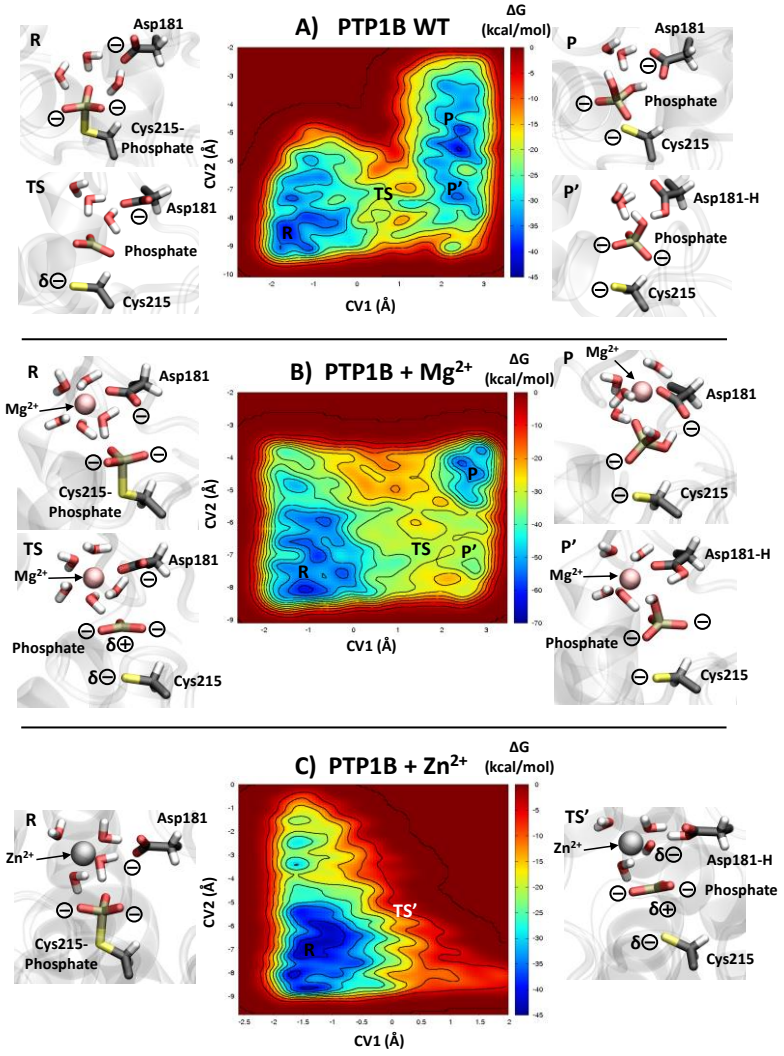

Figure 5. Free-energy surfaces for the PTP1B-catalyzed reaction in (A) the absence of ions; WT = wild type with Gln262 in place, in the presence of (B) Mg^{2+} and (C) Zn^{2+} ions, reconstructed from the metadynamics calculation as a function of the two CVs defined in the main text. The energy is given in kcal/mol. CV values are expressed in Ångströms. Each iso-line corresponds to 5 kcal/mol.

The PTP1B catalyzed-reaction in the presence of a bound Mg^{2+} proceeds through a similar mechanism. However, the FES displays some differences in the energy contours, especially in the product regions, where only one energy minimum was observed (Figure 5B). In particular, the presence of the positively charged Mg^{2+} stabilizes the transfer of a proton from Asp181 to the hydrolyzed phosphate, with only

product P observed during the metadynamics simulation. The product (P) resulting from the transfer of an additional proton from Asp181 to the hydrolyzed phosphate is approximately 24 kcal/mol higher in stability than P'. The reaction is exothermic with a total free energy change of 6 kcal/mol and a free energy barrier of 23 kcal/mol (Table S6). The observation of a higher energy barrier compared to the reaction without Mg^{2+} bound indicates a reaction differing from the experimental reports showing Mg^{2+}-dependent activation of PTP1B activity. The difference ($\Delta\Delta G$) in the pathways in the absence and presence of Mg^{2+} was 3 kcal/mol, while the difference in barrier heights ($\Delta\Delta G^{\ddagger}$) was 5 kcal/mol, indicative of only a small preference for the reaction in the absence of Mg^{2+} and suggestive of competition between the two mechanisms.

Magnesium is intricately linked to phosphate ester hydrolysis.[34] The free magnesium ion concentration in the cell is about 0.5 mM with dissociation constants of protein-Mg^{2+} complexes in the range of 0.1 to 1 mM.[34] Hence the effect of Mg^{2+} on PTP1B with an effector constant of 41 µM (Figure 1) is highly significant for the function of the enzyme in vivo. In other words, while Mg^{2+} is not considered to be part of the reaction mechanism of PTP1B established by crystal structures, the fact that magnesium ions are present in cells at concentrations causing activation indicates that PTP1B will employ Mg^{2+} as cofactor in the cell. It has been noted that positions of Mg^{2+} in crystal structures of proteins are difficult to ascertain because it is 'a small ion that is hard to discriminate from water', unless the crystallographic resolution is rather high.[35] The affinity of Mg^{2+} to a single phosphate is not very high and binding must be stabilized by negatively charged groups such as Asp181 in PTP1B. Mg^{2+} has octahedral coordination in contrast to zinc which is more flexible and adopts tetrahedral coordination and inhibits many Mg^{2+}-dependent enzymes. Analysis of FES of the PTP1B reaction in the presence of Zn^{2+} in a TS-like conformation highlights the inhibition as the reaction was unable to proceed (Figure 5C). This high-energy structure has a similar conformation to the one observed for the TS of the reaction of PTP1B in the presence of Mg^{2+} with a trigonal bipyramidal geometry of the phosphate group. Proton transfer from a water molecule to the acid/base residue Asp181 leads to the formation of a hydroxide bound to Zn^{2+}. The high affinity of Zn^{2+} for the negatively charged hydroxide ligand[33,36] prevents the nucleophilic attack of a water molecule and, therefore, product formation, presumably due to the prohibitive cost of desolvation of tetrahedral zinc compared to the cost of desolvation of octahedral magnesium. This is reflected in the lower energy barrier for the reaction in the presence of magnesium (23 kcal/mol) compared to zinc (30 kcal/mol).

In summary, consistent explanations are provided for the inhibitory effect of Zn^{2+} in the reaction mechanism of tyrosine phosphatases at the atomic level. The findings demonstrate remarkable differences in the structural enzymology of PTP1B investigated individually ex vivo and the function of the enzyme in vivo, where different reaction pathways become viable when the cellular concentrations of metal ions

and the interaction with the insulin receptor are considered. Mg^{2+} and Zn^{2+} are delivered to the active site of PTP1B via its substrate. For the function of the insulin receptor and its signalling, on which zinc has an insulin-mimetic effect[28] the results suggest a dual function of PTP1B with regard to zinc, namely activating the receptor by removing inhibitory zinc[30] and then becoming zinc-inhibited itself.

ASSOCIATED CONTENT

Supporting Information. (1) Fluorescence of phosphorylated insulin receptor peptides; (2) table of simulations performed; (3) representative illustrations of the MD systems; (4) parameters for the phosphorylated Tyr group; (5) schematic representation of the protocol followed to investigate the Zn^{2+}/Mg^{2+} coordination to PTP1B in the cysteinylphosphate intermediate; (5) geometries of the active site of the cysteinylphosphate intermediate upon geometry optimization of reactants and TS for Mg^{2+} and Zn^{2+} systems; (6) table with free-energy values obtained from metadynamics runs for the PTP1B enzymatic reaction; (7) comparison between active site catalytic residues and water molecules in the crystal structures, and representative snapshots from MD simulations. This material is available free of charge via the Internet at http://pubs.acs.org.

AUTHOR INFORMATION

Corresponding Authors:

*C.Domene@bath.ac.uk & wolfgang.maret@kcl.ac.uk

Current address:

Asma Abro, Department of Biotechnology, Balochistan University of Information Technology Engineering and Management Sciences (BUITEMS), Quetta, Pakistan.

Funding Sources

This work was supported by the Biotechnology and Biological Sciences Research Council (BB/L01825X/1 and BB/K001442/1). A.A. was supported by the Higher Education Commission of Pakistan through a scholarship under the ‘International Research Support Initiative Program’.

ACKNOWLEDGMENTS

The results of this research have been achieved using the DECI resource Archer based in the UK at EPCC, Marconi based in CINECA in Italy, and SuperMUC based in Jülich in Germany with support from PRACE.

ABBREVIATIONS

CGenFF, general force field; DFT, density functional theory; DiFMUP, 6,8-difluoro-4-methylumbelliferyl phosphate; FES, free energy surface; IR, insulin receptor; MD, molecular dynamics; NTA, nitrilotriacetic acid; PTPs, protein tyrosine phosphatases; TS, transition state.

References

1. Hammes, G. G., Multiple Conformational Changes in Enzyme Catalysis. *Biochemistry* **2002,** *41* (26), 8221-8228.
2. Brandão, T. A. S.; Hengge, A. C.; Johnson, S. J., Insights into the Reaction of Protein-tyrosine Phosphatase 1B: Crystal structures for transition state analogs of both catalytic steps. *J Biol Chem* **2010,** *285* (21), 15874-15883.
3. Denu, J. M.; Tanner, K. G., Specific and Reversible Inactivation of Protein Tyrosine Phosphatases by Hydrogen Peroxide: Evidence for a Sulfenic Acid Intermediate and Implications for Redox Regulation. *Biochemistry* **1998,** *37* (16), 5633-5642.
4. Alhambra, C.; Wu, L.; Zhang, Z.-Y.; Gao, J., Walden-Inversion-Enforced Transition-State Stabilization in a Protein Tyrosine Phosphatase. *J Am Chem Soc* **1998,** *120* (16), 3858-3866.
5. Pannifer, A. D. B.; Flint, A. J.; Tonks, N. K.; Barford, D., Visualization of the Cysteinyl-phosphate Intermediate of a Protein-tyrosine Phosphatase by X-ray Crystallography. *J Biol Chem* **1998,** *273* (17), 10454-10462.
6. Asthagiri, D.; Liu, T.; Noodleman, L.; Van Etten, R. L.; Bashford, D., On the Role of the Conserved Aspartate in the Hydrolysis of the Phosphocysteine Intermediate of the Low Molecular Weight Tyrosine Phosphatase. *Journal of the American Chemical Society* **2004,** *126* (39), 12677-12684.
7. Brautigan, D. L.; Bornstein, P.; Gallis, B., Phosphotyrosyl-protein phosphatase. Specific inhibition by Zn. *J Biol Chem* **1981,** *256* (13), 6519-6522.
8. Bellomo, E.; Massarotti, A.; Hogstrand, C.; Maret, W., Zinc ions modulate protein tyrosine phosphatase 1B activity. *Metallomics* **2014,** *6* (7), 1229-1239.
9. Wilson, M.; Hogstrand, C.; Maret, W., Picomolar concentrations of free zinc(II) ions regulate receptor protein-tyrosine phosphatase β activity. *J Biol Chem* **2012,** *287* (12), 9322-9326.
10. Barr, A. J.; Ugochukwu, E.; Lee, W. H.; King, O. N. F.; Filippakopoulos, P.; Alfano, I.; Savitsky, P.; Burgess-Brown, N. A.; Müller, S.; Knapp, S., Large-Scale Structural Analysis of the Classical Human Protein Tyrosine Phosphatome. *Cell 136* (2), 352-363.
11. Phillips, J. C.; Braun, R.; Wang, W.; Gumbart, J.; Tajkhorshid, E.; Villa, E.; Chipot, C.; Skeel, R. D.; Kale, L.; Schulten, K., Scalable molecular dynamics with NAMD. *J Comput Chem* **2005,** *26* (16), 1781-1802.
12. MacKerell, A. D.; Bashford, D.; Bellott, M.; Dunbrack, R. L.; Evanseck, J. D.; Field, M. J.; Fischer, S.; Gao, J.; Guo, H.; Ha, S.; Joseph-McCarthy, D.; Kuchnir, L.; Kuczera, K.; Lau, F. T. K.; Mattos, C.; Michnick, S.; Ngo, T.; Nguyen, D. T.; Prodhom, B.; Reiher, W. E.; Roux, B.; Schlenkrich, M.; Smith, J. C.; Stote, R.; Straub, J.; Watanabe, M.; Wiorkiewicz-Kuczera, J.; Yin, D.; Karplus, M., All-atom empirical potential for molecular modeling and dynamics studies of proteins. *J Phys Chem B* **1998,** *102* (18), 3586-3616.
13. Jorgensen, W. L.; Chandrasekhar, J.; Madura, J. D.; Impey, R. W.; Klein, M. L., Comparison of simple potential functions for simulating liquid water. *J Chem Phys* **1983,** *79* (2), 926-935.
14. Vanommeslaeghe, K.; Hatcher, E.; Acharya, C.; Kundu, S.; Zhong, S.; Shim, J.; Darian, E.; Guvench, O.; Lopes, P.; Vorobyov, I.; MacKerell, A. D., CHARMM General Force Field: A Force Field for Drug-Like Molecules Compatible with the CHARMM All-Atom Additive Biological Force Fields. *J Comput Chem* **2010,** *31* (4), 671-690.
15. Mayne, C. G.; Saam, J.; Schulten, K.; Tajkhorshid, E.; Gumbart, J. C., Rapid Parameterization of Small Molecules Using the Force Field Toolkit. *J Comput Chem* **2013,** *34* (32), 2757-2770.
16. Feller, S. E.; Zhang, Y. H.; Pastor, R. W.; Brooks, B. R., Constant-Pressure Molecular-Dynamics Simulation - the Langevin Piston Method. *J Chem Phys* **1995,** *103* (11), 4613-4621.
17. Martyna, G. J.; Tobias, D. J.; Klein, M. L., Constant-Pressure Molecular-Dynamics Algorithms. *J Chem Phys* **1994,** *101* (5), 4177-4189.
18. Izaguirre, J. A.; Catarello, D. P.; Wozniak, J. M.; Skeel, R. D., Langevin stabilization of molecular dynamics. *J Chem Phys* **2001,** *114* (5), 2090-2098.
19. Darden, T.; York, D.; Pedersen, L., Particle Mesh Ewald - an N.Log(N) Method for Ewald Sums in Large Systems. *J Chem Phys* **1993,** *98* (12), 10089-10092.
20. Laio, A.; Parrinello, M., Escaping free-energy minima. *P Natl Acad Sci USA* **2002,** *99* (20), 12562-12566.
21. Laino, T.; Mohamed, F.; Laio, A.; Parrinello, M., An Efficient Real Space Multigrid QM/MM Electrostatic Coupling. *J Chem Theory Comput* **2005,** *1* (6), 1176-1184.
22. Schafer, A.; Huber, C.; Ahlrichs, R., Fully Optimized Contracted Gaussian-Basis Sets of Triple Zeta Valence Quality for Atoms Li to Kr. *J Chem Phys* **1994,** *100* (8), 5829-5835.
23. Goedecker, S.; Teter, M.; Hutter, J., Separable dual-space Gaussian pseudopotentials. *Phys Rev B* **1996,** *54* (3), 1703-1710.
24. Hartwigsen, C.; Goedecker, S.; Hutter, J., Relativistic separable dual-space Gaussian pseudopotentials from H to Rn. *Phys Rev B* **1998,** *58* (7), 3641-3662.
25. Becke, A. D., Density-Functional Exchange-Energy Approximation with Correct Asymptotic-Behavior. *Phys Rev A* **1988,** *38* (6), 3098-3100.
26. Lee, C. T.; Yang, W. T.; Parr, R. G., Development of the Colle-Salvetti Correlation-Energy Formula into a Functional of the Electron-Density. *Phys Rev B* **1988,** *37* (2), 785-789.
27. Maseras, F.; Morokuma, K., Imomm - a New Integrated Ab-Initio Plus Molecular Mechanics Geometry Optimization Scheme of Equilibrium Structures and Transition-States. *J Comput Chem* **1995,** *16* (9), 1170-1179.
28. Bellomo, E.; Birla Singh, K.; Massarotti, A.; Hogstrand, C.; Maret, W., The metal face of protein tyrosine phosphatase 1B. *Coordination Chem Rev* **2016,** *327*, 70-83.
29. Harder, E.; MacKerell, A. D.; Roux, B., Many-Body Polarization Effects and the Membrane Dipole Potential. *J Am Chem Soc* **2009,** *131* (8), 2760-2761.

30. Pang, D. T.; Shafer, J. A., Inhibition of the activation and catalytic activity of insulin receptor kinase by zinc and other divalent metal ions. *J Biol Chem* **1985,** *260* (8), 5126-30.
31. Whittier, S. K.; Hengge, A. C.; Loria, J. P., Conformational Motions Regulate Phosphoryl Transfer in Related Protein Tyrosine Phosphatases. *Science* **2013,** *341* (6148), 899-903.
32. Desamero, R.; Rozovsky, S.; Zhadin, N.; McDermott, A.; Callender, R., Active Site Loop Motion in Triosephosphate Isomerase: T-Jump Relaxation Spectroscopy of Thermal Activation. *Biochemistry* **2003,** *42* (10), 2941-2951.
33. Dudev, T.; Lim, C., Competition among Metal Ions for Protein Binding Sites: Determinants of Metal Ion Selectivity in Proteins. *Chem Rev* **2014,** *114* (1), 538-556.
34. Cowan, J. A., Metal-mediated hydrolysis of biological phosphate esters. *JBIC Journal of Biological Inorganic Chemistry* **1997,** *2* (2), 168-176.
35. Braun, W.; Schein, C. H., Membrane Interaction and Functional Plasticity of Inositol Polyphosphate 5-Phosphatases. *Structure* **2014,** *22* (5), 664-666.
36. Dudev, T.; Lim, C., Principles Governing Mg, Ca, and Zn Binding and Selectivity in Proteins. *Chem Rev* **2003,** *103* (3), 773-788.

Authors are required to submit a graphic entry for the Table of Contents (TOC) that, in conjunction with the manuscript title, should give the reader a representative idea of one of the following: A key structure, reaction, equation, concept, or theorem, etc., that is discussed in the manuscript. Consult the journal's Instructions for Authors for TOC graphic specifications.